Journal of Magnetic Resonance **151,** 85–89 (2001)
doi:10.1006/jmre.2001.2360, available online at http://www.idealibrary.com on IDEAL®

Improving Resolution in Fast Rotating-Frame Experiments

F. Casanova, H. Robert,[1] and D. Pusiol

Facultad de Matemática, Astronomía y Física, Universidad Nacional de Córdoba, Ciudad Universitaria, 5000 Córdoba, Argentina

Received December 8, 2000; revised April 10, 2001

The rapid rotating-frame technique allows significant reduction in data-acquisition time compared with the two-dimensional method by stroboscopic observation of the nuclear magnetization during its evolution in the rotating frame. A onefold reduction in the dimensionality of the original rotating-frame experiment is achieved by using a train of strong radiofrequency pulses separated by short acquisition windows. The penalty for shortening experimental time is a reduction in spectral resolution compared with the two-dimensional method due to relaxation of transverse magnetization components during the observation windows. A variant of the rapid-rotating frame technique for improving spectral resolution based on undersampling and self-phase encoding is presented. An *M*-fold resolution improvement requires *M* experiments, thus, making possible a tradeoff between spectral resolution and experimental time. The technique was applied for spatial localization of quadrupole nuclei in powder solids, and resolution improvement is demonstrated on one- and two-dimensional NQR images.

Key Words: **rotating-frame imaging; nutation spectroscopy; NQR imaging.**

INTRODUCTION

In rotating-frame spin localization experiments, the spatial information is encoded by using radiofrequency (RF) field B_1 gradients; i.e., the variation in the RF amplitude across the sample encodes the spin spatial coordinates along the axis of the RF gradient. The original rotating-frame spatial encoding method (*1*) involves a two-dimensional experiment for obtaining a one-dimensional spin-density profile. Free-induction decay signals are measured for various excitation pulse lengths and the spatial frequencies are sampled through the amplitude or phase modulation of the spin magnetization. Acquisition of an N-point nutation signal takes about $3 \times T_1 \times N$ because complete recovery of the equilibrium spin population is necessary between experiments. In this experiment, spatial resolution is determined by the relaxation time T_{12} that occurs during the application of the encoding RF pluse (*2*).

The rapid rotating-frame method allows one to image a one-dimensional spin-density projection along the RF field gradient axis in a single experiment (*2–5*). The technique involves magnetization sampling in the course of nutation induced by a train of short RF pulses, of length Δt_1, applied with an inhomogeneous B_1 field, and separated by short acquisition intervals τ of free evolution. The time interval τ allows recovery of the receiver and sampling of the magnetization components. Acquisition of an N-point nutation signal takes about $N \times (\Delta t_1 + \tau)$, which is much shorter than the spin–lattice relaxation parameter T_1. Therefore, this method reduces data-acquisition time in a 1D imaging experiment by a factor of about $T_1/(\Delta t_1 + \tau)$, in comparison with the two-dimensional technique.

When applying the rapid rotating-frame method on solids (*4, 5*), we encountered a reduction in spatial resolution compared with the 2D encoding technique. This is because the effective decay of the nutation signal T_{2e} as a function of the advance of the encoding process is now given by T_2 during each interval τ of free evolution in addition to the decay T_{12} during RF pulses of length Δt_1. Assuming exponential decays of the magnetization, the effective relaxation time during the rapid rotating-frame method can be expressed as

$$\frac{1}{T_{2e}} = \frac{1}{T_R}\left(\frac{\Delta t_1}{T_{12}} + \frac{\tau}{T_2}\right),$$

where $T_R = \tau + \Delta t_1$ is the period of the pulse train. The time decay constant T_{2e} defines the linewidth of the point response function that determines the spatial resolution.

To obtain the highest resolution in rotating-frame imaging experiments one uses the maximal amplitude of the radiofrequency field gradient $G_{1,\max}$, which is limited by the available RF power and the geometry of the gradient coil. In the technique with stroboscopic signal acquisition, the duration of the pulses Δt_1 determines the spectral width $S_W = \pi/\Delta t_1$. Therefore, the sampling interval of the nutation signal defines the Nyquist bandwidth for an imaging projection or field of view S_X which is given by

$$S_X = \frac{S_w}{\gamma k G_{1,\max}}. \qquad [1]$$

The parameter $k = \sqrt{(I+m)(I-m+1)}/2$ depends on the

[1] Present address: Quantum Magnetics, 7740 Kenamar Court, San Diego, CA 92121.

1090-7807/01 $35.00

spin number I and the transition $m \leftrightarrow (m-1)$ being excited. For example, for a spin $I = 3/2$ quadrupole system $k = \sqrt{3}/2$.

The field of view S_X should be adapted to the size of the object L to avoid aliasing of spatial frequencies. This imposes the condition

$$\Delta t_{1,\max} = \frac{\pi}{\gamma k G_{1,\max} L}, \qquad [2]$$

for the maximal sampling interval $\Delta t_{1,\max}$. The maximal number of signal samplings that can be made before the signal decays out is roughly given by the ratio T_{2e}/T_R. Then, for a given object length L, the highest spatial resolution Δ_X attainable with $G_{1,\max}$ and $\Delta t_{1,\max}$ is

$$\Delta_X = \frac{L}{\pi}\frac{T_R}{T_{2e}} = \frac{L}{\pi}\left(\frac{\Delta t_{1,\max}}{T_{12}} + \frac{\tau}{T_2}\right). \qquad [3]$$

The last equation shows that the penalty for using acquisition windows is a loss of resolution due to the effects of relaxation T_2 during τ.

The pulse train for the rapid nutation experiment uses RF duty cycles, $\Delta t_1/\tau$, not higher than 20–30% and T_2 is shoter than the relaxation time during the RF pulse T_{12}. Then the spatial resolution is mainly dictated by the decay T_2 during the acquisition interval τ and is given by

$$\Delta_X = \frac{L}{\pi}\frac{\tau}{T_2}. \qquad [4]$$

The ultimate resolution does not depend on the B_1-field gradient but is determined by τ/T_2, which corresponds to the maximal number of signal samplings. Therefore, to increase resolution under a given T_2 the observation window should be reduced but, in practice, τ is limited by the finite deadtime of the receiver.

In this work, we describe a variant of the 1D rotating-frame experiment to improve the spatial resolution, beyond the limit dictated by the relaxation decay T_2, without significant increase in experimental time. The technique is based on undersampling of the nutation signal to improve spectral resolution, and self-phase encoding to avoid aliasing. Undersampling of the signal is a useful trick for improving digital resolution in an indirect dimension by deliberately increasing the sampling time. If the sampling interval Δt_1 is increased by a factor M, the resolution is $1/M$ times better, but the reduced spectral width $\pi/M\Delta t_1$ can cause aliasing. This problem is overcomed by using self-phase encoding (*6*).

Let us discuss first the approach to achieve a twofold increase in spatial resolution, $M = 2$. Figure 1a shows the encoding sequence that is applied with pulses twice as long as the required sampling interval $\Delta t_1 = 2\Delta t_{1,\max}$ and the number of pulses is $N/2$. The first pulse of the sequence acts as a preparatory pulse and its length is varied in successive experiments to shift the nutation signal, or pseudo-FID, in the time domain t_1. Two $N/2$-point pseudo-FIDs are acquired in separate experiments and the width of the preparatory pulse is $\Delta t_{1,\max}$ and $2\Delta t_{1,\max}$. Then the first experiment samples the evolution of the magnetization in the rotating frame at time intervals $(2n-1)\Delta t_{1,\max}$ and the second experiment at the values $2n\Delta t_{1,\max}$, for $n = 1, \ldots, (N/2)$. By superimposing the two pseudo-FIDs, shifted by $\Delta t_{1,\max}$ with respect to each other, an N-point signal sampled at the intervals $\Delta t_{1,\max}$ is obtained as shown in Fig. 1b. The resulting spatial resolution is now given by

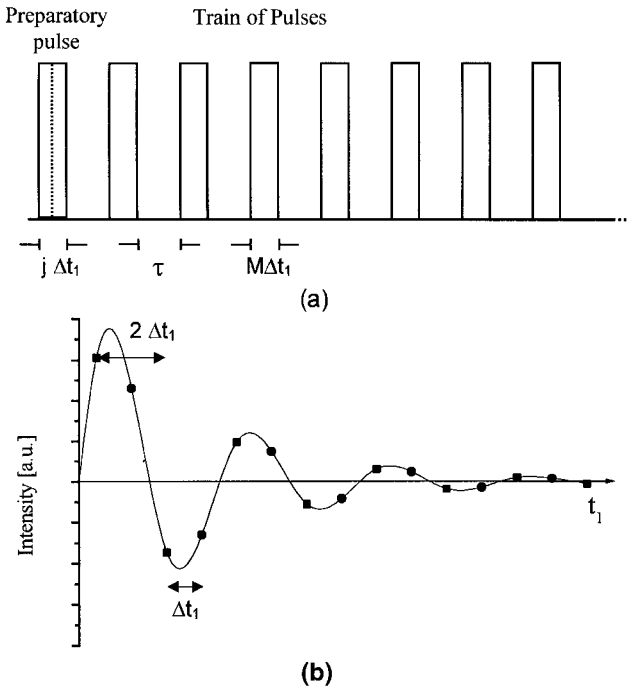

FIG. 1. (a) Pulse sequence to improve resolution in the rapid-rotating frame technique. The sampling interval in the pulse-width time domain is deliberately increased by a factor of $M = 2$. The length of the preparatory pulse Δt_p is increased in successive experiments, $\Delta t_p = j\Delta t_1$ $(j = 1, 2)$, thus shifting the nutation signals in steps of Δt_1 in the time domain t_1. (b) The phase-shifted nutation signals superimposed to yield a nutation signal whose sampling interval is now Δt_1. Therefore, the resulting sampling interval is Δt_1 and the acquisition window is artificially reduced to $\tau/2$.

$$\Delta_X = \frac{L}{\pi}\frac{\tau}{2T_2},$$

and a twofold improvement in spatial discrimination is obtained.

For a general application of our variant of the rapid-rotating frame technique, the nutation signal is undersampled by the train of N/M pulses with length $M\Delta t_{1,\max}$ and acquisition window τ. A preparatory pulse is introduced to shift the nutation signal in the time domain t_1, and its length Δt_p is increased M times in successive experiments, $\Delta t_p = j\Delta t_{1,\max}$ $(j = 1, \ldots, M)$. A set of M phase-shifted nutation signals is recorded and superimposed to yield an interleaved nutation signal whose sampling interval is now $\Delta t_{1,\max}$. Therefore, the resulting spectral width is $\pi/\Delta t_{1,\max}$ but the acquisition interval is artificially reduced to

τ/M, thus improving the spatial resolution. This variant of the rapid rotating-frame experiment increases the experimental time by a factor $M \times T_1$. The technique yields a noticeable resolution improvement until the ratio τ/MT_2 is comparable to the ratio $\Delta t_{1,\max}/T_{12}$.

EXPERIMENTS AND RESULTS

To demonstrate the improvement in spatial resolution using the technique described above, one- and two-dimensional NQR localization experiments were carried out on powder samples. The experiments were performed on our homemade NQR spectrometer described elsewhere (*4, 7*). A three-turn surface coil of 24 mm diameter delivered the RF gradient and was also used for signal detection. The measured strength of the encoding RF gradient was 30 G/cm at the position of the object. The resonant circuit was tuned at 34.260 MHz, the ^{35}Cl resonance of paradichlorobenzene at room temperature.

To compare the resolution achieved with the conventional rapid rotating-frame technique and that with the self-phase encoding variant, one-dimensional profiles were acquired using both methods. The test object consisted of two cylindrical layers of powder paradichlorobenzene, 8 mm diameter and 2.5 mm thickness, separated by a 2.5-mm-thick spacer. The object was aligned along the axis of the surface coil and positioned in the region of an approximately constant RF gradient (between 0.2 and 0.9 of the coil's radius). Reconstruction of the spatial profiles for the powder sample from the nutation signals was performed by the maximum-entropy method (MEM) as described in previous papers (*8, 9*). The spectral amplitudes were corrected according to the B_1-field profile to account for the spatial sensitivity dependence of the receiver coil.

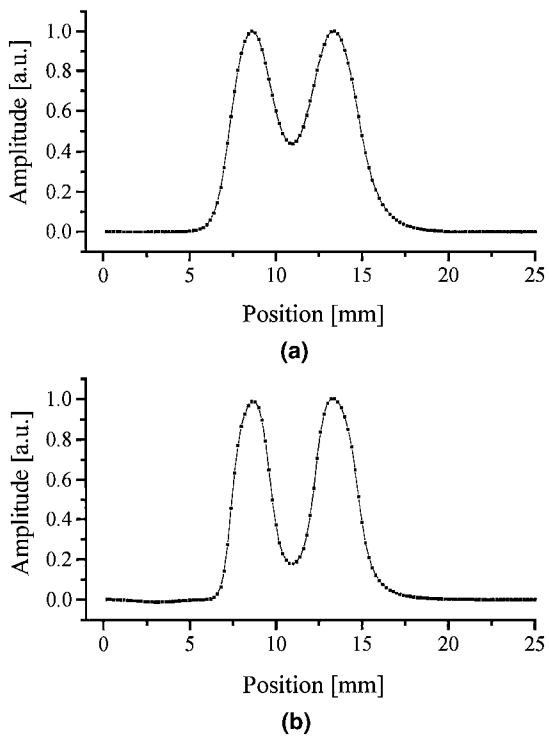

FIG. 2. One-dimensional spatial distributions from a test object of powder paradichlorobenzene consisting of two disks of 2.5 mm thickness separated by a 2.5-mm spacer. Profiles acquired with the conventional rapid rotating-frame technique (a) and a twofold self-phase-encoding method (b) were reconstructed by MEM, and peak intensities were corrected to account for the spatial sensitivity dependence of the receiver coil.

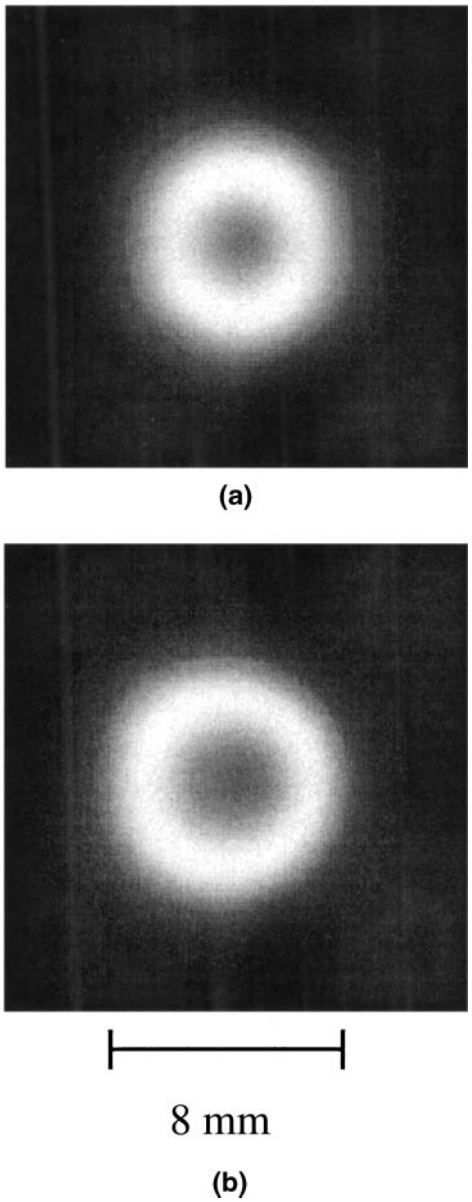

FIG. 3. Cross-section NQR images obtained by the filtered back-projection–reconstruction procedure. The object is a cylinder of polycrystalline paradichlorobenzene of 8 mm diameter with a central hole of 4 mm inner diameter. The cross-section images were reconstructed from a set of 50 projections acquired with the conventional rapid rotating-frame method (a) and with a twofold self-phase-encoding procedure (b).

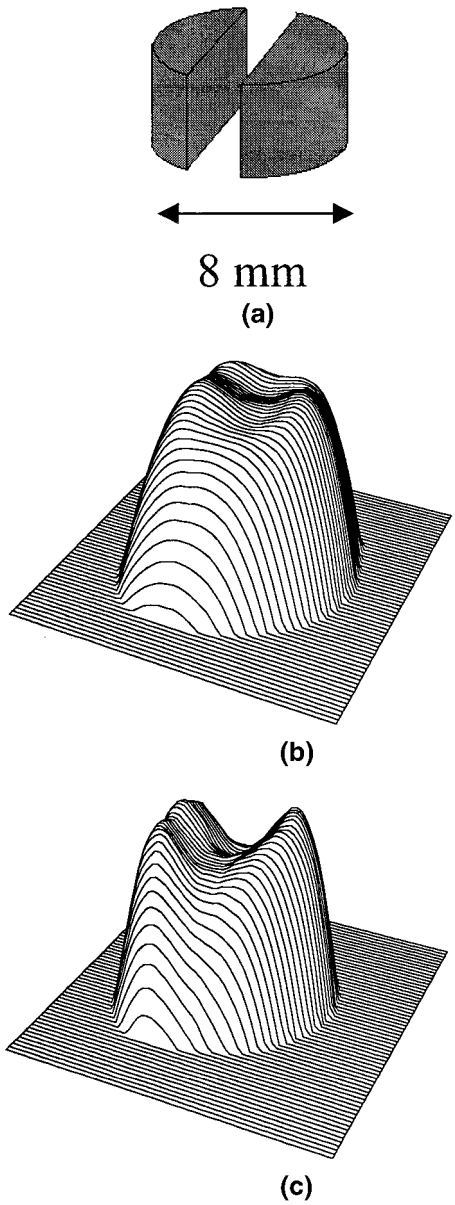

FIG. 4. Stack plots showing the two-dimensional projection of the test object of powder paradichlorobenzene with the geometry depicted in (a). (b) Two-dimensional projection recorded with the single-scan rotating-frame method. (c) Cross-section image obtained with a twofold self-phase-encoding technique.

In the rapid rotating-frame experiment, the nutation signal was acquired with a train of 64 RF pulses, $\Delta t_1 = 10\,\mu$s, separated by a detection interval τ of 40 μs. Figure 2a shows the 128-point density profile reconstructed by MEM. For a twofold resolution improvement, pseudo-FIDs were acquired with a train of 32 pulses, 20 μs width, and acquisition windows of 40 μs. Preparatory pulses of 10 and 20 μs were used to acquire two time-shifted nutation signals that were combined as shown in Fig. 1b. The resulting 64-point signal has a sampling interval of 10 μs and a slower decay that leads to the apparent higher resolution in the reconstructed profile (Fig. 2b).

Two-dimensional NQR images were obtained by the conventional projection–reconstruction technique. To map a cross section of the powder sample, the object was rotated around an axis perpendicular to the RF gradient in a step-by-step manner by means of a suitable mechanical device (*10*). For each technique, a set of 50 pseudo-FIDs was recorded for different orientations of the sample relative to the RF gradient delivered by the surface coil. The 2D images were then reconstructed from the MEM-reconstructed projections by means of the filtered-back-projection algorithm (*10*). Parameters of the pulse sequences were identical to those used on the one-dimensional experiments described above.

Two different cross-section geometries were used to compare the techniques with and without resolution improvement. Figure 3 shows the reconstructed cross-section images from a cylinder of 8 mm diameter with a hole in the center of 4 mm inner diameter. The image reconstructed from data acquired with the conventional rapid rotating-frame technique (Fig. 3a) does not reproduce the actual dimensions of the object due to the lower resolution of the method. Figure 3b shows the 2D image obtained with the new version of the rotating-frame method implemented to give a twofold improvement in resolution. Figure 4 shows the stack plot of the 2D projections for a cylindrical object of 8 mm diameter with a rectangular spacer of 2 mm thickness introduced in the middle (Fig. 4a). Projections were obtained with the same experimental parameters used for the first object. The 3D view of the cross-section images shows clearly the resolution improvement obtained with the new version of the technique (Fig. 4c) compared with that of the conventional method (Fig. 4b).

CONCLUSIONS

We presented a new variant of the rapid rotating-frame encoding method for reducing the effective acquisition windows, leading to an improvement in the spatial resolution of the technique. The proposed technique was tested by mapping one-dimensional profiles and two-dimensional distributions of quadrupole nuclei in powder samples. The simplest version for twofold reduction of observation windows yields a noticeable resolution enhancement compared with that of the conventional single-shot rotating-frame method in our solid samples. The drawback of the proposed technique is that the experimental time increases by a factor of about $3 \times T_1 \times M$, where M is the number of self-phase encoding steps or reduction in effective acquisition windows. However, the technique is still a factor of M/N faster than the conventional 2D method. With samples having short transverse relaxation time T_2 the two-dimensional method yields the highest resolution. Although the technique is here demonstrated on NQR imaging experiment, it can be directly applied to rotating-frame NMR (*2*) and nutation NQR spectroscopy for determination of the asymmetry parameter on spin-$\frac{3}{2}$ systems (*11*).

ACKNOWLEDGMENTS

We thank the National Agency of Science and Technique (ANPCYT) and the National and Provincial Research Councils (CONICET and CONICOR) for financial support. F.C. thanks CONICET for the research fellowship.

REFERENCES

1. D. I. Hoult, *J. Magn. Reson.* **33,** 183 (1979).
2. P. Maffei, P. Mutzenhardt, A. Retournard, B. Diter, R. Raulet, J. Brondeau, and D. Canet, *J. Magn. Reson. A* **107,** 40 (1994).
3. F. Humbert, B. Diter, and D. Canet, *J. Magn. Reson. A* **123,** 242 (1996).
4. H. Robert, A. Minuzzi, and D. Pusiol, *J. Magn. Reson. A* **118,** 189 (1996).
5. F. Casanova, H. Robert, and D. Pusiol, *J. Magn. Reson.* **141,** 62 (1999).
6. S. Matsui, A. Uraoka, and T. Inouye, *J. Magn. Reson. A* **112,** 130 (1995).
7. H. Robert and D. Pusiol, *Z. Naturforsch. A* **51,** 353 (1996).
8. E. Rommel, R. Kimmich, H. Robert, and D. Pusiol, *Meas. Sci. Technol.* **3,** 446 (1992).
9. H. Robert, D. Pusiol, E. Rommel, and R. Kimmich, *Z. Naturforsch. A* **49,** 35 (1994).
10. P. Nickel, E. Rommel, R. Kimmich, and D. Pusiol, *Chem. Phys. Lett.* **183,** 183 (1991).
11. H. Robert and D. Pusiol, *J. Chem. Phys.* **106,** 2096 (1997).